J.Natn.Sci.Foundation Sri Lanka 2025 53 (4): 363 - 373
DOI: http://dx.doi.org/10.4038/jnsfsr.v53i4.12405

RESEARCH ARTICLE

Magnetism

Magnetic properties of body-centred cubic ferromagnetic thin films described by the fourth order perturbed Heisenberg Hamiltonian

MSM Farhan[1*] and P Samarasekara[2]
Department of Physical Science, Facalty of Applied Science, Trincomalee Campus, Eastern University, Sri Lanka.
Department of Physics, Facalty of Science, University of Peradeniya, Peradeniya, Sri Lanka.

Submitted: 21 October 2024; Revised: 11 November 2025; Accepted: 27 November 2025

Abstract: This research investigates the magnetic properties of body-centred cubic (bcc) ferromagnetic thin films with three spin layers, using a detailed model known as the fourth-order perturbed Heisenberg Hamiltonian. Ferromagnetic thin films are essential for modern technologies, such as magnetic sensors and spintronic devices, because their magnetic behaviour can be precisely controlled. We investigated the influence of magnetic anisotropy and spin exchange interactions on the spatial distribution of magnetic energy across the layers. Using MATLAB simulations, we created 3-D and 2-D graphs to analyse energy in relation to the spin exchange interaction and azimuthal angle. Our results show that the total magnetic energy can vary significantly, reaching orders of 10^{17} when the fourth-order anisotropy constant in the bottom spin layer is minimized. In contrast, when the middle spin layer has lower anisotropy, the total magnetic energy decreases to the order of 10^{13}, indicating that it becomes easier for the magnetic moments to rotate. We also found that the angle between consecutive magnetic easy and hard directions is not always 90 degrees, and interchanging layers leads to slight changes in energy maxima and minima. Importantly, the total magnetic energy is significantly higher in configurations with two spin layers, ranging from 10^{42} to 10^{43}, compared to those with three layers. These results underscore the sensitivity of bcc ferromagnetic thin films to variations in magnetic anisotropy and provide important insights for future applications in magnetic storage, sensors, and spintronic technologies.

Keywords: Fourth order perturbed Heisenberg Hamiltonian, magnetic anisotropy constant, magnetic thin films, Spin exchange interaction, spin layers.

INTRODUCTION

Ferromagnetic thin films are important for many modern technologies, such as hard drives, magnetic sensors, and spintronics devices. These films are valuable because their magnetic properties can be controlled at very small scales. The behaviour of these films depends on various factors like interactions between spins, magnetic anisotropy (which defines the preferred direction of magnetization), dipole interactions, and external magnetic fields. Among these materials, thin films with a body-centred cubic (bcc) structure are particularly interesting due to their unique atomic arrangement. In films with three spin layers, the magnetic properties can be complex, as each layer behaves differently based on how the spins interact and align. A key factor that influences their behaviour is magnetic anisotropy, which determines the direction in which the material is easiest to magnetize. Other factors like stress and dipole interactions also play a big role in the magnetic properties of these films.

To understand these properties, researchers often use the Heisenberg Hamiltonian model, which takes into account interactions between spins and the effects of magnetic anisotropy. In previous studies, simpler versions of this model were used to describe thin film magnetism, but for a more detailed analysis, we apply the fourth-order perturbed Heisenberg Hamiltonian.

* Corresponding author (farhanmsm@esn.ac.lk; https://orcid.org/0009-0001-8708-9460)

This version of the model includes higher-order effects like second and fourth-order anisotropy, which helps us better understand how magnetic energy changes across the different spin layers.

Ferromagnetic materials have a natural magnetization, meaning they maintain a magnetic moment even without an external magnetic field. This happens because the spins of electrons are arranged in a regular pattern within regions called magnetic domains. The spin exchange interaction between atoms causes the magnetic moments to align. If the spin exchange constant (J) is positive, the moments align parallel, but if J is negative, they align in opposite directions (antiparallel). Above a certain temperature, called the Curie temperature, the magnetization disappears, and the material becomes paramagnetic. At higher temperatures, the magnetic behaviour follows the Curie-Weiss law. Ferromagnetism comes from unpaired electron spins in the outer subshells of atoms. However, the measured magnetic moments of materials often differ from theoretical predictions due to subshell overlap. When a magnetic field is applied, magnetization increases as spins in different domains rotate and domain walls move. In thin magnetic films, stress can affect magnetization during the heating and cooling process (annealing) because of differences in thermal expansion between the film and its substrate. This stress-induced magnetic anisotropy is similar in strength to the material's natural magneto-crystalline anisotropy, and it influences the material's coercivity, which is a measure of its resistance to becoming demagnetized (Samarasekara & Cadieu, 2001a, 2001b).

Ferromagnetic films have been studied using various models. For example, Monte Carlo simulations have been used to explore the magnetic hysteresis (how magnetization changes with applied magnetic fields) in ferromagnetic thin films grown on special substrates (Zhao *et al.*, 2002). The Ising model has been applied to study the magnetic properties of films with alternating layers (Bentaleb *et al.*, 2002). Additionally, the structural and magnetic properties of two-dimensional FeCo alloys have been determined using first-principles band structure theory (Spisak & Hafner, 2005). The magnetic behaviour of nickel layers on copper has also been studied using the Korringa-Kohn-Rostoker Green's function method (Ernst *et al.*, 2000).

In this manuscript, the total magnetic energy of ferromagnetic thin films is described by solving the classical Heisenberg Hamiltonian. This approach considers all relevant energy terms, including magnetic energy, spin dipole interaction energy, spin exchange interaction energy, second and fourth-order magnetic anisotropy constants, stress-induced anisotropy, and the demagnetization factor. The fourth-order perturbed Heisenberg Hamiltonian, incorporating all seven magnetic energy parameters, is explained for the bcc structure with three spin layers. MATLAB software was used to plot 3-D and 2-D graphs of energy as a function of spin exchange interaction and the azimuthal angle of the spin. The main objective of this study is to investigate how variations in the anisotropy constants of different spin layers influence the magnetic energy minima and maxima in bcc structure ferromagnetic thin films. This helps clarify how layer-dependent anisotropy affects the overall magnetic stability and behaviour of these films.

MODEL

The Heisenberg Hamiltonian of ferromagnetic films can be formulated as follows (Samarasekara *et al.*, 2009, Samarasekara & De Silva, 2007, Samarasekara, 2008).

$$H = -\frac{J}{2}\sum_{m,n} \vec{S}_m.\vec{S}_n + \frac{\omega}{2}\sum_{m\neq n}\left(\frac{\vec{S}_m.\vec{S}_n}{r_{mn}^3} - \frac{3(\vec{S}_m.\vec{r}_{mn})(\vec{r}_{mn}.\vec{S}_n)}{r_{mn}^5}\right)$$

$$-\sum_m D_{\lambda_m}^{(2)}(S_m^z)^2 - \sum_m D_{\lambda_m}^{(4)}(S_m^z)^4$$

$$-\sum_{m,n}[\vec{\boldsymbol{H}} - (\boldsymbol{N_d}\vec{\boldsymbol{S}}_n/\boldsymbol{\mu_0})].\vec{\boldsymbol{S}}_m - \sum_m \boldsymbol{K_s}\,\boldsymbol{sin\,2\theta_m} \quad ...(01)$$

Here $\vec{S}_m$ and $\vec{S}_n$ are two spins. The above equation can be simplified into the following form

$$E(\theta) = -\frac{1}{2}\sum_{m,n=1}^{N}\left[\left(JZ_{|m-n|} - \frac{\omega}{4}\Phi_{|m-n|}\right)\cos(\theta_m - \theta_n) - \frac{3\omega}{4}\Phi_{|m-n|}\cos(\theta_m + \theta_n)\right]$$

$$-\sum_{m=1}^{N}(D_m^{(2)}cos^2\theta_m + D_m^{(4)}cos^4\theta_m + H_{in}sin\theta_m + H_{out}cos\theta_m) + \sum_{m,n=1}^{N}\frac{N_d}{\mu_0}cos(\theta_m - \theta_n)$$

$$-K_s\sum_{m=1}^{N} sin2\theta_m \quad ...(02)$$

Here N, $m\ (or\ n)$, J, $Z_{|m-n|}$, ω, $\Phi_{|m-n|}$, $\theta_m(\theta_n)$, $D_m^{(2)}$, $D_m^{(4)}$, H_{in}, H_{out}, N_d and K_s are the total number of layers, layer index, spin exchange interaction, number of nearest spin neighbors, strength of long range dipole interaction, partial summations of dipole interaction, azimuthal angles of spins, second and fourth order anisotropy constants, in plane and out of plane applied magnetic fields, demagnetization factor, and stress induced anisotropy constants, respectively.

The spin structure is considered to be slightly disoriented. Therefore, the spins could be considered to have angles distributed about an average angle θ. By choosing azimuthal angles as

$\theta_m = \theta + \varepsilon_m$ and $\theta_n = \theta + \varepsilon_n$ ...(03)

Where the ε's are small positive or negative angular deviations,

Then, $\theta_m - \theta_n = \varepsilon_m - \varepsilon_n$ and $\theta_m + \theta_n = 2\theta + \varepsilon_m + \varepsilon_n$ ...(04)

Substituting equations (3) and (4) in the classical Heisenberg Hamiltonian (2), results in

$$E(\theta) = -\frac{1}{2}\sum_{m,n=1}^{N}\left[\left(JZ_{|m-n|} - \frac{\omega}{4}\Phi_{|m-n|}\right)\cos(\varepsilon_m - \varepsilon_n) - \frac{3\omega}{4}\Phi_{|m-n|}\cos(2\theta + \varepsilon_m + \varepsilon_n)\right] - \sum_{m=1}^{N}(D_m^{(2)}cos^2(\theta + \varepsilon_m)$$
$$+ D_m^{(4)}cos^4(\theta + \varepsilon_m) + H_{in}sin(\theta + \varepsilon_m) + H_{out}cos(\theta + \varepsilon_m)) + \sum_{m,n=1}^{N}\frac{N_d}{\mu_0}cos(\varepsilon_m - \varepsilon_n) - K_s\sum_{m=1}^{N}sin2(\theta + \varepsilon_m) \quad ...(05)$$

The cosine and sine terms can be expanded up to the fourth order of $\varepsilon_m\varepsilon_m$ and $\varepsilon_n\varepsilon_n$ as following.

$$E(\theta) = E_0 + E(\varepsilon) + E(\varepsilon^2) + E(\varepsilon^3) + E(\varepsilon^4) \quad ...(06)$$

Here,

$$E_0 = -\frac{1}{2}\sum_{m,n=1}^{N}\left(JZ_{|m-n|} - \frac{\omega}{4}\Phi_{|m-n|}\right) + \frac{3\omega}{8}cos2\theta\sum_{m,n=1}^{N}\Phi_{|m-n|} - cos^2\theta\sum_{m=1}^{N}D_m^{(2)} - cos^4\theta\sum_{m=1}^{N}D_m^{(4)} - N(H_{in}sin\theta$$
$$+ H_{out}cos\theta + K_s sin2\theta) + \frac{N_d N^2}{\mu_0} \quad ...(07)$$

$$E(\varepsilon) = -\frac{3\omega}{8}sin2\theta\sum_{m,n=1}^{N}\Phi_{|m-n|}(\varepsilon_m + \varepsilon_n) + sin2\theta\sum_{m=1}^{N}D_m^{(2)}\varepsilon_m + 2cos^2\theta sin2\theta\sum_{m=1}^{N}D_m^{(4)}\varepsilon_m - H_{in}cos\theta\sum_{m=1}^{N}\varepsilon_m$$
$$+ H_{out}sin\theta\sum_{m=1}^{N}\varepsilon_m - 2K_s cos2\theta\sum_{m=1}^{N}\varepsilon_m \quad ...(08)$$

$$E(\varepsilon^2) = \frac{1}{4}\sum_{m,n=1}^{N}\left(JZ_{|m-n|} - \frac{\omega}{4}\Phi_{|m-n|}\right)(\varepsilon_m - \varepsilon_n)^2 - \frac{3\omega}{16}cos2\theta\sum_{m,n=1}^{N}\Phi_{|m-n|}(\varepsilon_m + \varepsilon_n)^2 + cos2\theta\sum_{m=1}^{N}D_m^{(2)}\varepsilon_m^2$$
$$+ 2cos^2\theta(cos^2\theta - 3sin^2\theta)\sum_{m=1}^{N}D_m^{(4)}\varepsilon_m^2 + \frac{H_{in}}{2}sin\theta\sum_{m=1}^{N}\varepsilon_m^2 + \frac{H_{out}}{2}cos\theta\sum_{m=1}^{N}\varepsilon_m^2 - \frac{N_d}{2\mu_0}\sum_{m,n=1}^{N}(\varepsilon_m - \varepsilon_n)^2 + 2K_s sin2\theta\sum_{m=1}^{N}\varepsilon_m^2 \quad ...(09)$$

$$E(\varepsilon^3) = \frac{\omega}{16} sin2\theta \sum_{m,n=1}^{N} \Phi_{|m-n|} (\varepsilon_m + \varepsilon_n)^3 - \frac{4}{3} sin\theta cos\theta \sum_{m=1}^{N} D_m^{(2)} \varepsilon_m^3 \ -4 sin\theta cos\theta \left(\frac{5}{3} cos^2\theta - sin^2\theta\right) \sum_{m=1}^{N} D_m^{(4)} \varepsilon_m^3$$

$$+ \frac{H_{in}}{6} cos\theta \sum_{m=1}^{N} \varepsilon_m^3 - \frac{H_{out}}{6} sin\theta \sum_{m=1}^{N} \varepsilon_m^3 \ + \frac{4}{3} K_s cos2\theta \sum_{m=1}^{N} \varepsilon_m^3 \qquad ...(10)$$

$$E(\varepsilon^4) = -\frac{1}{48} \sum_{m,n=1}^{N} \left(JZ_{|m-n|} - \frac{\omega}{4} \Phi_{|m-n|}\right) (\varepsilon_m - \varepsilon_n)^4 + \frac{\omega}{64} cos2\theta \sum_{m,n=1}^{N} \Phi_{|m-n|} (\varepsilon_m + \varepsilon_n)^4 \ - \frac{1}{3} cos2\theta \sum_{m=1}^{N} D_m^{(2)} \varepsilon_m^4$$

$$- \left(\frac{5}{3} cos^4\theta - 8 cos^2\theta sin^2\theta + sin^4\theta\right) \sum_{m=1}^{N} D_m^{(4)} \varepsilon_m^4 \ - \frac{H_{in}}{24} sin\theta \sum_{m=1}^{N} \varepsilon_m^4 - \frac{H_{out}}{24} cos\theta \sum_{m=1}^{N} \varepsilon_m^4$$

$$+ \frac{N_d}{24\mu_0} \sum_{m,n=1}^{N} (\varepsilon_m - \varepsilon_n)^4 \ - \frac{2}{3} K_s sin2\theta \sum_{m=1}^{N} \varepsilon_m^4 \qquad ...(11)$$

For films with three spin layers, $N = 3$. Therefore, m and n change from 1 to 3.

$$E_0 = -\frac{3}{2}\left(JZ_0 - \frac{\omega}{4}\Phi_0\right) - 2\left(JZ_1 - \frac{\omega}{4}\Phi_1\right) + \frac{3\omega}{8} cos2\theta (3\Phi_0 + 4\Phi_1) - cos^2\theta (D_1^{(2)} + D_2^{(2)} + D_3^{(2)})$$

$$-cos^4\theta \left(D_1^{(4)} + D_2^{(4)} + D_3^{(4)}\right) - 3(H_{in} sin\theta + H_{out} cos\theta + K_s sin2\theta) + 9\frac{N_d}{\mu_0} \qquad ...(12)$$

$$E(\varepsilon) = -\frac{3\omega}{4} sin2\theta [\Phi_0(\varepsilon_1 + \varepsilon_2 + \varepsilon_3) + \Phi_1(\varepsilon_1 + 2\varepsilon_2 + \varepsilon_3)] + sin2\theta (D_1^{(2)}\varepsilon_1 + D_2^{(2)}\varepsilon_2 + D_3^{(2)}\varepsilon_3)$$

$$+2cos^2\theta sin2\theta \left(D_1^{(4)}\varepsilon_1 + D_2^{(4)}\varepsilon_2 + D_3^{(4)}\varepsilon_3\right) - H_{in} cos\theta (\varepsilon_1 + \varepsilon_2 + \varepsilon_3) + H_{out} sin\theta (\varepsilon_1 + \varepsilon_2 + \varepsilon_3)$$

$$-2K_s cos2\theta (\varepsilon_1 + \varepsilon_2 + \varepsilon_3) \qquad ...(13)$$

$$E(\varepsilon^2) = \frac{1}{2}\left(JZ_1 - \frac{\omega}{4}\Phi_1\right)({\varepsilon_1}^2 + 2{\varepsilon_2}^2 + {\varepsilon_3}^2 - 2\varepsilon_1\varepsilon_2 - 2\varepsilon_2\varepsilon_3) - \frac{3\omega}{8} cos2\theta [2\Phi_0({\varepsilon_1}^2 + {\varepsilon_2}^2 + {\varepsilon_3}^2)$$

$$+\Phi_1({\varepsilon_1}^2 + 2{\varepsilon_2}^2 + {\varepsilon_3}^2 + 2\varepsilon_1\varepsilon_2 + 2\varepsilon_2\varepsilon_3)] + cos2\theta (D_1^{(2)}{\varepsilon_1}^2 + D_2^{(2)}{\varepsilon_2}^2 \ + D_3^{(2)}{\varepsilon_3}^2)$$

$$+2cos^2\theta (cos^2\theta - 3sin^2\theta)\left(D_1^{(4)}{\varepsilon_1}^2 + D_2^{(4)}{\varepsilon_2}^2 + D_3^{(4)}{\varepsilon_3}^2\right) + \frac{H_{in}}{2} sin\theta ({\varepsilon_1}^2 + {\varepsilon_2}^2 + {\varepsilon_3}^2)$$

$$+\frac{H_{out}}{2} cos\theta ({\varepsilon_1}^2 + {\varepsilon_2}^2 + {\varepsilon_3}^2) - 2\frac{N_d}{\mu_0}({\varepsilon_1}^2 + {\varepsilon_2}^2 + {\varepsilon_3}^2 - \varepsilon_1\varepsilon_2 - \varepsilon_1\varepsilon_3 - \varepsilon_2\varepsilon_3)$$

$$+2K_s sin2\theta ({\varepsilon_1}^2 + {\varepsilon_2}^2 + {\varepsilon_3}^2) \qquad ...(14)$$

$$E(\varepsilon^3) = \frac{\omega}{8} sin2\theta[4\Phi_0({\varepsilon_1}^3 + {\varepsilon_2}^3 + {\varepsilon_3}^3) + \Phi_1({\varepsilon_1}^3 + 3{\varepsilon_1}^2\varepsilon_2 + 3\varepsilon_1{\varepsilon_2}^2 + 2{\varepsilon_2}^3 + 3{\varepsilon_2}^2\varepsilon_3 + 3\varepsilon_2{\varepsilon_3}^2 + {\varepsilon_3}^3)]$$

$$-\frac{4}{3} sin\theta cos\theta \left(D_1^{(2)}{\varepsilon_1}^3 + D_2^{(2)}{\varepsilon_2}^3 + D_3^{(2)}{\varepsilon_3}^3\right) - 4sin\theta cos\theta \left(\frac{5}{3}cos^2\theta - sin^2\theta\right)$$

$$\left(D_1^{(4)}{\varepsilon_1}^3 + D_2^{(4)}{\varepsilon_2}^3 + D_3^{(4)}{\varepsilon_3}^3\right) + \frac{H_{in}}{6} cos\theta({\varepsilon_1}^3 + {\varepsilon_2}^3 + {\varepsilon_3}^3) - \frac{H_{out}}{6} sin\theta({\varepsilon_1}^3 + {\varepsilon_2}^3 + {\varepsilon_3}^3)$$

$$+\frac{4}{3} K_s cos2\theta({\varepsilon_1}^3 + {\varepsilon_2}^3 + {\varepsilon_3}^3) \quad ...(15)$$

$$E(\varepsilon^4) = -\frac{1}{24}\left(JZ_1 - \frac{\omega}{4}\Phi_1\right)({\varepsilon_1}^4 - 4{\varepsilon_1}^3\varepsilon_2 + 6{\varepsilon_1}^2{\varepsilon_2}^2 - 4\varepsilon_1{\varepsilon_2}^3 + 2{\varepsilon_2}^4 - 4{\varepsilon_2}^3\varepsilon_3 + 6{\varepsilon_2}^2{\varepsilon_3}^2$$

$$-4\varepsilon_2{\varepsilon_3}^3 + {\varepsilon_3}^4) + \frac{\omega}{32} cos2\theta[8\Phi_0({\varepsilon_1}^4 + {\varepsilon_2}^4 + {\varepsilon_3}^4) + \Phi_1({\varepsilon_1}^4 + 4{\varepsilon_1}^3\varepsilon_2 + 6{\varepsilon_1}^2{\varepsilon_2}^2$$

$$+4\varepsilon_1{\varepsilon_2}^3 + 2{\varepsilon_2}^4 + 4{\varepsilon_2}^3\varepsilon_3 + 6{\varepsilon_2}^2{\varepsilon_3}^2 + 4\varepsilon_2{\varepsilon_3}^3 + {\varepsilon_3}^4)] - \frac{1}{3} cos2\theta(D_1^{(2)}{\varepsilon_1}^4 + D_2^{(2)}{\varepsilon_2}^4$$

$$+D_3^{(2)}{\varepsilon_3}^4) - \left(\frac{5}{3}cos^4\theta - 8cos^2\theta sin^2\theta + sin^4\theta\right)\left(D_1^{(4)}{\varepsilon_1}^4 + D_2^{(4)}{\varepsilon_2}^4 + D_3^{(4)}{\varepsilon_3}^4\right)$$

$$-\frac{H_{in}}{24} sin\theta({\varepsilon_1}^4 + {\varepsilon_2}^4 + {\varepsilon_3}^4) - \frac{H_{out}}{24} cos\theta({\varepsilon_1}^4 + {\varepsilon_2}^4 + {\varepsilon_3}^4) + \frac{N_d}{6\mu_0}({\varepsilon_1}^4 - 2{\varepsilon_1}^3\varepsilon_2 + 3{\varepsilon_1}^2{\varepsilon_2}^2$$

$$-2\varepsilon_1{\varepsilon_2}^3 + {\varepsilon_2}^4 - 2{\varepsilon_1}^3\varepsilon_3 + 3{\varepsilon_1}^2{\varepsilon_3}^2 - 2\varepsilon_1{\varepsilon_3}^3 + {\varepsilon_3}^4 - 2{\varepsilon_2}^3\varepsilon_3 + 3{\varepsilon_2}^2{\varepsilon_3}^2$$

$$-2\varepsilon_2{\varepsilon_3}^3) - \frac{2}{3} K_s sin2\theta({\varepsilon_1}^4 + {\varepsilon_2}^4 + {\varepsilon_3}^4) \quad ...(16)$$

The first order perturbation term can be expressed in terms of a row and column matrix with all seven terms in each, as follows.

$$E(\varepsilon) = \vec{\alpha}.\vec{\varepsilon} \quad ...(17)$$

Here the terms of α are given by α_1, α_2 and α_3.

$$\alpha_1 = -\frac{3\omega}{4} sin2\theta(\Phi_0 + \Phi_1) + sin2\theta D_1^{(2)} + 2cos^2\theta sin2\theta D_1^{(4)} - H_{in}cos\theta + H_{out}sin\theta - 2K_s cos2\theta \quad ...(18)$$

$$\alpha_2 = -\frac{3\omega}{4} sin2\theta(\Phi_0 + 2\Phi_1) + sin2\theta D_2^{(2)} + 2cos^2\theta sin2\theta D_2^{(4)} - H_{in}cos\theta + H_{out}sin\theta - 2K_s cos2\theta \quad ...(19)$$

$$\alpha_3 = -\frac{3\omega}{4} sin2\theta(\Phi_0 + \Phi_1) + sin2\theta D_3^{(2)} + 2cos^2\theta sin2\theta D_3^{(4)} - H_{in}cos\theta + H_{out}sin\theta - 2K_s cos2\theta \quad ...(20)$$

The second order perturbation term can be expressed in terms of a 2 × 2 × 2 matrix, a row matrix and a column matrix, as follows.

$$E(\varepsilon^2) = \frac{1}{2}\vec{\varepsilon}.C.\vec{\varepsilon} \quad ...(21)$$

Elements of the 3 × 3 matrix (*C*) are delineated by

$$C_{11} = JZ_1 - \frac{\omega}{4}\Phi_1 - \frac{3\omega}{4}cos2\theta(2\Phi_0 + \Phi_1) + 2cos2\theta D_1^{(2)} + 4cos^2\theta(cos^2\theta - 3sin^2\theta)D_1^{(4)} + H_{in}sin\theta + H_{out}cos\theta - \frac{4N_d}{\mu_0} + 4K_s sin2\theta \quad ...(22)$$

$$C_{12} = C_{21} = C_{23} = C_{32} = -JZ_1 + \frac{\omega}{4}\Phi_1 - \frac{3\omega}{4}cos2\theta\Phi_1 + \frac{2N_d}{\mu_0} \quad ...(23)$$

$$C_{13} = C_{31} = \frac{2N_d}{\mu_0} \quad ...(24)$$

$$C_{22} = 2\left(JZ_1 - \frac{\omega}{4}\Phi_1\right) - \frac{3\omega}{2}cos2\theta(\Phi_0 + \Phi_1) + 2cos2\theta D_2^{(2)} + 4cos^2\theta(cos^2\theta - 3sin^2\theta)D_2^{(4)} + H_{in}sin\theta + H_{out}cos\theta - \frac{4N_d}{\mu_0} + 4K_s sin2\theta \quad ...(25)$$

$$C_{33} = JZ_1 - \frac{\omega}{4}\Phi_1 - \frac{3\omega}{4}cos2\theta(2\Phi_0 + \Phi_1) + 2cos2\theta D_3^{(2)} + 4cos^2\theta(cos^2\theta - 3sin^2\theta)D_3^{(4)} + H_{in}sin\theta + H_{out}cos\theta - \frac{4N_d}{\mu_0} + 4K_s sin2\theta \quad ...(26)$$

The third order perturbation term can be expressed in terms of a 2 × 2 matrix, a row matrix and a column matrix, as follows.

$$E(\varepsilon^3) = \varepsilon^2.\beta.\vec{\varepsilon} \quad ...(27)$$

Elements of the 3 × 3 matrix (*β*) are specified by

$$\beta_{11} = \frac{\omega}{8}sin2\theta(4\Phi_0 + \Phi_1) - \frac{4}{3}sin\theta cos\theta D_1^{(2)} - 4sin\theta cos\theta\left(\frac{5}{3}cos^2\theta - sin^2\theta\right)D_1^{(4)} + \frac{H_{in}}{6}cos\theta - \frac{H_{out}}{6}sin\theta + \frac{4}{3}K_s cos2\theta \quad ...(28)$$

$$\beta_{12} = \beta_{21} = \beta_{23} = \beta_{32} = \frac{3\omega}{8}sin2\theta\Phi_1 \quad ...(29)$$

$$\beta_{13} = \beta_{31} = 0 \quad ...(30)$$

$$\beta_{22} = \frac{\omega}{4}sin2\theta(2\Phi_0 + \Phi_1) - \frac{4}{3}sin\theta cos\theta D_2^{(2)} - 4sin\theta cos\theta\left(\frac{5}{3}cos^2\theta - sin^2\theta\right)D_2^{(4)} + \frac{H_{in}}{6}cos\theta - \frac{H_{out}}{6}sin\theta + \frac{4}{3}K_s cos2\theta \quad ...(31)$$

$$\beta_{33} = \frac{\omega}{8}sin2\theta(4\Phi_0 + \Phi_1) - \frac{4}{3}sin\theta cos\theta D_3^{(2)} \cdot - 4sin\theta cos\theta\left(\frac{5}{3}cos^2\theta - sin^2\theta\right)D_3^{(4)} + \frac{H_{in}}{6}cos\theta - \frac{H_{out}}{6}sin\theta + \frac{4}{3}K_s cos2\theta \quad ...(32)$$

The fourth order perturbation term can be expressed in terms of a 2 × 2 matrix, a row matrix and a column matrix, as follows.

$$E(\varepsilon^4) = \varepsilon^3.F.\vec{\varepsilon} + \varepsilon^2.G.\varepsilon^2 \quad ...(33)$$

Elements of the 3 × 3 matrix (*F* and *G*) are delineated by

$$F_{11} = -\frac{1}{24}\left(JZ_1 - \frac{\omega}{4}\Phi_1\right) + \frac{\omega}{32}cos2\theta(8\Phi_0 + \Phi_1) - \frac{1}{3}cos2\theta D_1^{(2)} - \left(\frac{5}{3}cos^4\theta - 8cos^2\theta sin^2\theta + sin^4\theta\right) D_1^{(4)} - \frac{H_{in}}{24}sin\theta - \frac{H_{out}}{24}cos\theta + \frac{N_d}{6\mu_0} - \frac{2}{3}K_s sin2\theta \quad ...(34)$$

$$D_1^{(4)} - \frac{H_{in}}{24}sin\theta - \frac{H_{out}}{24}cos\theta + \frac{N_d}{6\mu_0} - \frac{2}{3}K_s sin2\theta$$
...(34)

$$F_{21} = F_{23} = F_{32} = \frac{1}{6}\left(JZ_1 - \frac{\omega}{4}\Phi_1\right) + \frac{\omega}{8}cos2\theta\Phi_1 - \frac{N_d}{3\mu_0}$$
...(35)

$$F_{13} = F_{31} = -\frac{N_d}{3\mu_0}$$
...(36)

$$F_{22} = -\frac{1}{12}\left(JZ_1 - \frac{\omega}{4}\Phi_1\right) + \frac{\omega}{16}cos2\theta(4\Phi_0 + \Phi_1)$$

$$-\frac{1}{3}cos2\theta D_2^{(2)} - \left(\frac{5}{3}cos^4\theta - 8cos^2\theta sin^2\theta + sin^4\theta\right)$$

$$D_2^{(4)} - \frac{H_{in}}{24}sin\theta - \frac{H_{out}}{24}cos\theta + \frac{N_d}{6\mu_0} - \frac{2}{3}K_s sin2\theta$$
...(37)

$$F_{33} = -\frac{1}{24}\left(JZ_1 - \frac{\omega}{4}\Phi_1\right) + \frac{\omega}{32}cos2\theta(8\Phi_0 + \Phi_1)$$

$$-\frac{1}{3}cos2\theta D_3^{(2)} - \left(\frac{5}{3}cos^4\theta - 8cos^2\theta sin^2\theta + sin^4\theta\right)$$

$$D_3^{(4)} - \frac{H_{in}}{24}sin\theta - \frac{H_{out}}{24}cos\theta + \frac{N_d}{6\mu_0} - \frac{2}{3}K_s sin2\theta$$
...(38)

$$G_{11} = G_{22} = G_{33} = 0$$
...(39)

$$G_{12} = G_{21} = -\frac{1}{8}\left(JZ_1 - \frac{\omega}{4}\Phi_1\right) + \frac{3\omega}{32}cos2\theta\Phi_1 + \frac{N_d}{4\mu_0}$$
...(40)

$$G_{23} = G_{32} = -\frac{1}{8}\left(JZ_1 - \frac{\omega}{4}\Phi_1\right) + \frac{3\omega}{32}cos2\theta\Phi_1 + \frac{N_d}{2\mu_0}$$
... (41)

$$G_{13} = G_{31} = \frac{N_d}{4\mu_0}$$
...(42)

Therefore, the total magnetic energy given in equation (6) can be deduced to

$$E(\theta) = E_0 + \vec{\alpha}.\vec{\varepsilon} + \frac{1}{2}\vec{\varepsilon}.C.\vec{\varepsilon} + \varepsilon^2.\beta.\vec{\varepsilon} + \varepsilon^3.F.\vec{\varepsilon} + \varepsilon^2.G.\varepsilon^2$$
...(43)

For the minimum energy of the second order perturbed term

$$\vec{\varepsilon} = -C^+.\alpha$$
...(45)

Here C^+ is the pseudo inverse of matrix C. C^+ can be found using

$$C.C^+ = 1 - \frac{E}{N}$$
...(45)

Here E is the matrix with all elements given *by* $E_{mn} = 1$. I is the identity matrix.
Therefore, from the matrix equation (44)

$$\varepsilon_1 = -(C_{11}^+\alpha_1 + C_{12}^+\alpha_2 + C_{13}^+\alpha_3)$$
...(46)

$$\varepsilon_2 = -(C_{21}^+\alpha_1 + C_{22}^+\alpha_2 + C_{23}^+\alpha_3)$$
...(47)

$$\varepsilon_3 = -(C_{31}^+\alpha_1 + C_{32}^+\alpha_2 + C_{33}^+\alpha_3)$$
...(48)

After substituting ε in equation (43), the total magnetic energy can be determined.

RESULTS AND DISCUSSION

All the graphs presented in this manuscript were generated for ferromagnetic thin films featuring a bcc lattice structure with three distinct spin layers. Specifically, for films with a bcc (001) orientation, the parameters used are as follows: $Z_0 = 4$, $Z_1 = 1$, $Z_2 = 0$ and $\Phi_0 = 9.0336$, $\Phi_1 = -0.3275$ as referenced in previous studies (Hucht & Usadel, 1997, Hucht & Usadel, 1999, Usadel & Hucht, 2002). These values correspond to key structural and magnetic characteristics of the bcc (001) films, influencing the overall magnetic behaviour and energy configurations analyzed in the simulations.

A 3-D plot of energy versus angle and spin exchange interaction is given in Figure 1 for $\frac{D_1^{(4)}}{\omega} = 5$, $\frac{D_2^{(4)}}{\omega} = 10$ and $\frac{D_3^{(4)}}{\omega} = 10$. Here other parameters are fixed at $\frac{H_{in}}{\omega} = \frac{H_{out}}{\omega} = \frac{N_d}{\mu_0\omega} = \frac{D_1^{(2)}}{\omega} = \frac{D_2^{(2)}}{\omega} = \frac{D_3^{(2)}}{\omega} = \frac{K_s}{\omega} = 10$ for this simulation. The peaks along the direction of the angle are closely packed compared to the second and third order perturbed cases (Samarasekara, 2006, Samarasekara *et al.*, 2009, Samarasekara, 2010, Samarasekara & Mendoza, 2010, Samarasekara, 2011). The energy maxima can be observed at $\frac{J}{\omega} =$ 2, 25, 50, 73. The major maximum is observed at about $\frac{J}{\omega} =$ 73. Energy in these graphs is in the order of 10^{17}. For bcc structured ferromagnetic thin films with two spin layers, the total magnetic energy reached 10^{35} (Farhan & Samarasekara, 2024). The total magnetic energy was significantly higher in the two spin layers for the same structure.

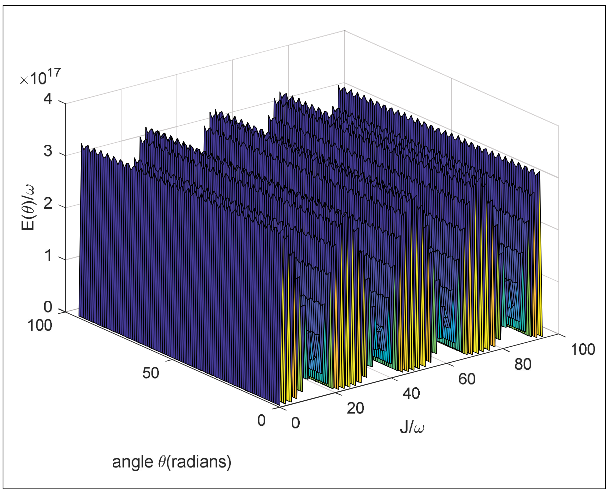

Figure 1: 3-D plot of energy versus angle and spin exchange interaction for $\frac{D_1^{(4)}}{\omega} = 5$, $\frac{D_2^{(4)}}{\omega} = 10$ and $\frac{D_3^{(4)}}{\omega} = 10$.

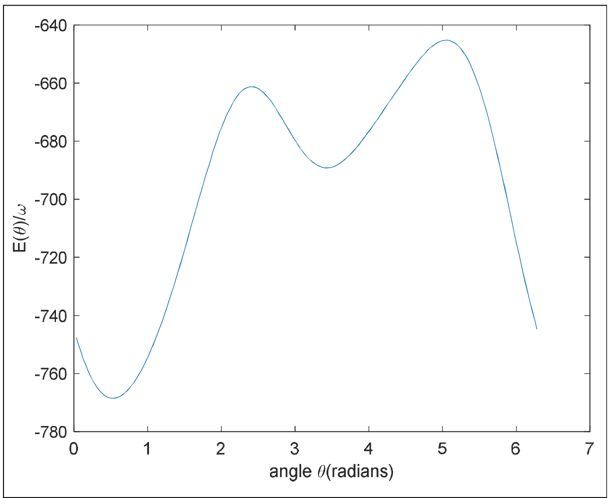

Figure 2: 2-D graph of energy versus angle

Figure 2 shows the graph of energy versus angle for $\frac{J}{\omega} =$ 73. In this graph, energy maxima are observed at 2.419 and 5.058 radians, with the major maximum occurring at around 5.058 radians. Energy minima are found at 0.5341 and 3.456 radians, with the major minimum at approximately 0.5341 radians. The angle between consecutive magnetic easy and hard directions is not 90 degrees. The shape of the graph differs from that observed in simple cubic structured ferromagnetic thin films with two spin layers (Farhan & Samarasekara, 2023).

Figures 3 represents the 3-D plot of energy versus angle and spin exchange interaction for $\frac{D_1^{(4)}}{\omega} = 10$, $\frac{D_2^{(4)}}{\omega} = 10$ and $\frac{D_3^{(4)}}{\omega} = 5$. Here other parameters are fixed at $\frac{H_{in}}{\omega} = \frac{H_{out}}{\omega} = \frac{N_d}{\mu_0\omega} = \frac{D_1^{(2)}}{\omega} = \frac{D_2^{(2)}}{\omega} = \frac{D_3^{(2)}}{\omega} = \frac{K_s}{\omega} = 10$ for this simulation. Energy maxima are observed at $\frac{J}{\omega} =$ 2, 19, 44, 67, 90, with the major maximum occurring at about $\frac{J}{\omega} = 67$. The energy values are in the order of 10^{14}. The total magnetic energy decreases when the bottom and top spin layers are interchanged, while the middle spin layer remains at a constant.

Figure 4 shows the graph of energy versus angle for $\frac{J}{\omega} = 67$. In this graph, energy maxima are observed at 2.356 and 5.058 radians, with the major maximum occurring around 5.058 radians. Energy minima are found at 0.5341 and 3.424 radians, with the major minimum at approximately 0.5341 radians. The angle between consecutive magnetic easy and hard directions is not 90 degrees. When compared to Figure 2, the maximum and minimum values change slightly when the bottom and top spin layers are interchanged, while the middle spin layer remains constant.

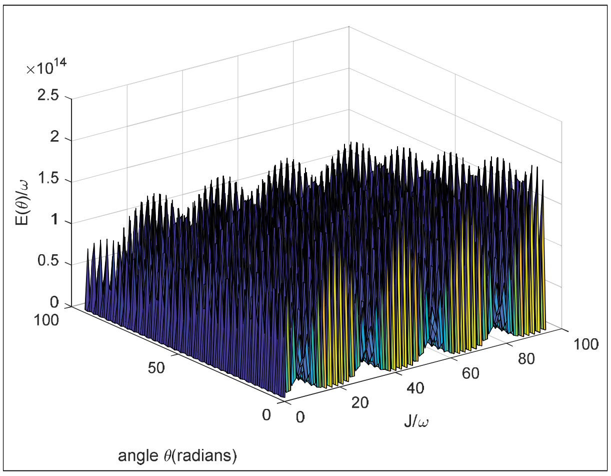

Figure 3: 3-D plot of energy versus angle and spin exchange interaction for $\frac{D_1^{(4)}}{\omega} = 10$, $\frac{D_2^{(4)}}{\omega} = 10$ and $\frac{D_3^{(4)}}{\omega} = 5$.

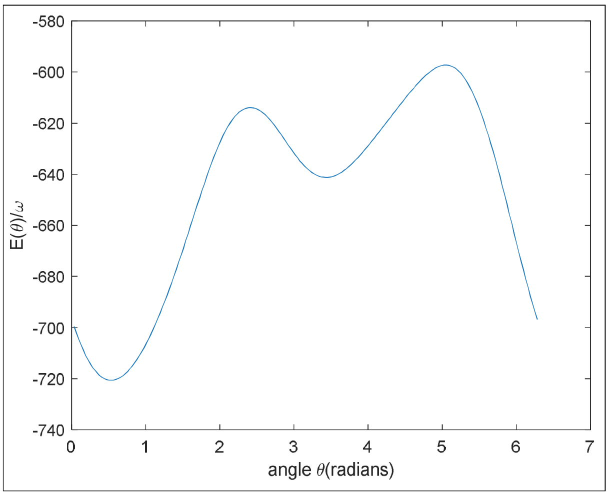

Figure 4: 2-D graph of energy versus angle

Figures 5 represents the 3-D plot of energy versus angle and spin exchange interaction for $\frac{D_1^{(4)}}{\omega} = 10$, $\frac{D_2^{(4)}}{\omega} = 5$ and $\frac{D_3^{(4)}}{\omega} = 10$. Here other parameters are fixed at $\frac{H_{in}}{\omega} = \frac{H_{out}}{\omega} = \frac{N_d}{\mu_0 \omega} = \frac{D_1^{(2)}}{\omega} = \frac{D_2^{(2)}}{\omega} = \frac{D_3^{(2)}}{\omega} = \frac{K_s}{\omega} = 10$ for this simulation. Energy maxima are observed at $\frac{J}{\omega} =$ 2, 23, 48, 71, with the major maximum occurring at about $\frac{J}{\omega} = 71$. Energy in these graphs is in the order of 10^{13}. The total magnetic energy decreases when the middle spin layer is smaller than the bottom and top spin layers. Comparing the 3-D plots in Figures 1, 3, and 5, the total energy ranges from 10^{13} to 10^{17}. Additionally, the energy maxima shift slightly when the values of the spin layers change. In the same structure with two spin layers, the total magnetic energy range is observed to be from 10^{42} to 10^{43}. It is clear that the total magnetic energy significantly changes as the number of spin layers increases for the same structure. The total magnetic energy in the 3-D graph of energy versus angle and stress induced anisotropy constant is to be observed from 10^{11} to 10^{21} with the same spin layer and structure (Farhan & Samarasekara, 2024). A lower energy gap is observed between the highest and lowest magnetic energy when changing the parameters for the same spin layer and structure.

Figure 6 shows the graph of energy versus angle for $\frac{J}{\omega} = 71$. In this graph, energy maxima are observed at 2.419 and 5.058 radians, with the major maximum occurring at approximately 5.341 radians. Energy minima are found at 0.5341 and 3.456 radians, with the major minimum at around 0.5341 radians. The angle between consecutive magnetic easy and hard directions is not 90 degrees. According to Figures 2 and 6, the maximum and minimum values remain unchanged when the bottom and middle spin layers are interchanged, while the top spin layer remains constant.

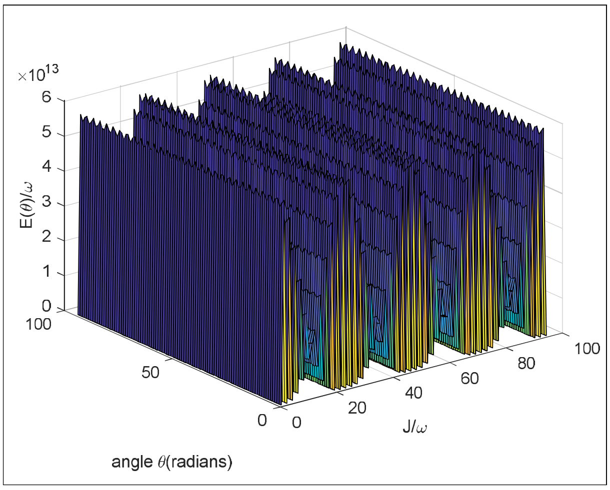

Figure 5: 3-D plot of energy versus angle and spin exchange interaction for $\frac{D_1^{(4)}}{\omega} = 10$, $\frac{D_2^{(4)}}{\omega} = 5$ and $\frac{D_3^{(4)}}{\omega} = 10$.

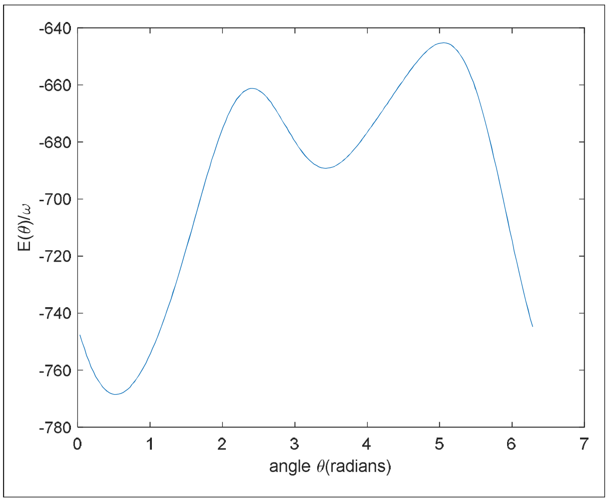

Figure 6: 2-D graph of energy versus angle

CONCLUSION

In conclusion, our study of bcc-structured ferromagnetic thin films with three spin layers, using the fourth-order perturbed Heisenberg Hamiltonian, has provided valuable insights into the magnetic energy distribution under varying parameter conditions. The findings reveal that when the fourth-order magnetic anisotropy constant in the bottom spin layer is smaller than those in the middle and top spin layers, the total magnetic energy reaches the order of 10^{17}. In contrast, when the middle spin layer has a lower fourth-order anisotropy constant, the total magnetic energy decreases to the order of 10^{13}. This indicates that a reduced fourth-order anisotropy in the middle spin layer leads to lower energy barriers for rotating magnetic moments away from the easy axis. Additionally, the energy maxima shift slightly with changes in the values of the spin layers. For comparison, in the same structure with two spin layers, the total magnetic energy was observed to range between 10^{42} and 10^{43}, showing that the total magnetic energy significantly decreases as the number of spin layers increases. A lower energy gap is also observed between the highest and lowest magnetic energies when altering the parameters for the same spin layer and structure. Furthermore, in the 2D plots, the angle between consecutive magnetic easy and hard directions is consistently not 90 degrees, and the maximum and minimum energy values remain unchanged when the bottom and middle spin layers are interchanged, while the top spin layer stays constant. This study highlights the sensitivity of the magnetic behaviour of bcc-structured ferromagnetic thin films to variations in the magnetic anisotropy constants and spin exchange interactions across different spin layers. Furthermore, we note that extending these simulations to systems with a larger number of spin layers (higher N) could provide deeper insights into the energy behaviour of ferromagnetic thin films. Since manual calculations become increasingly complex as N increases, future studies will employ MATLAB and other computational tools to explore these extended systems. These findings deepen our understanding of magnetic energy configurations in thin films and offer insights that could be beneficial for future applications in magnetic storage devices, sensors, and spintronic technologies.

REFERENCES

Bentaleb, M., Aouad El, N., & Saber, M. (2002). Exact solution of the one-dimensional Ising model in a random oscillating magnetic field. *Chinese Journal of Physics,* 40(3), 307.

Ernst, A., Lueders, M., Temmerman, W.M., *et al.* (2000). Theoretical study of magnetic layers of nickel on copper: dead or alive? *Journal of Physics: Condensed Matter,* 12(26), 5599–5606. https://doi.org/10.1088/0953-8984/12/26/306

Farhan, M.S.M., & Samarasekara, P. (2023). Simple cubic structured ferromagnetic thin films with two spin layers explained by fourth order perturbed Heisenberg Hamiltonian. *In Proceedings of the 4th International Conference on Applied & Pure Sciences (ICAPS)* (p. 65). University of Kelaniya, Sri Lanka.

Farhan, M.S.M., & Samarasekara, P. (2024). Determination of bcc structured ferromagnetic thin films with two spin layers using the fourth order perturbed Heisenberg Hamiltonian. *In Proceedings of the 2nd International Conference on Multidisciplinary Research (ICMR)* (p. 18). Eastern University, Sri Lanka. https://doi.org/10.4038/cjs.v52i2.8155

Farhan, M.S.M., & Samarasekara, P. (2024). Exploring magnetic anisotropy in bcc-structured ferromagnetic thin films with three spin layers using the fourth order perturbed Heisenberg Hamiltonian. *Georgian Electronic Scientific Journals: Physics,* 1(30), 6–19.

Hucht, A., & Usadel, K.D. (1997). Reorientation transition of ultrathin ferromagnetic films. *Physical Review B 55:* 12309. https://doi.org/10.1103/PhysRevB.55.12309

Hucht, A., & Usadel, K.D. (1999). Theory of the spin reorientation transition of ultra-thin ferromagnetic films. *Journal of Magnetism and Magnetic Materials 203(1):* 88-90. DOI: 10.1016/S0304-8853(99)00197-3. https://doi.org/10.1016/S0304-8853(99)00197-3

Samarasekara, P. & Mendoza, W.A. (2011). Third order perturbed Heisenberg Hamiltonian of spinel ferrite ultra-thin films. *Georgian Electronic Scientific Journals: Physics,* 1(5), 15–24.

Samarasekara, P. (2006). Second order perturbation of Heisenberg Hamiltonian for non-oriented ultra-thin ferromagnetic films. *Electronic Journal of Theoretical Physics,* 3(11), 71–83.

Samarasekara, P. (2008). Influence of third order perturbation on Heisenberg Hamiltonian of thick ferromagnetic films. *Electronic Journal of Theoretical Physics,* 5(17), 227–236.

Samarasekara, P. (2010). Determination of energy of thick spinel ferrite films using Heisenberg Hamiltonian with second order perturbation. *Georgian Electronic Scientific Journals: Physics, 1(3), 46–52.*

Samarasekara, P., & Cadieu, F.J. (2001). Magnetic and structural properties of RF sputtered polycrystalline lithium mixed ferrimagnetic films. *Chinese Journal of Physics,* 39(6), 635–640.

Samarasekara, P., & Cadieu, F.J. (2001). Polycrystalline Ni ferrite films deposited by RF sputtering techniques. *Japanese Journal of Applied Physics,* 40(5R), 3176. https://doi.org/10.1143/JJAP.40.3176

Samarasekara, P., & De Silva, S.N.P. (2007). Heisenberg Hamiltonian solution of thick ferromagnetic films with second order perturbation. *Chinese Journal of Physics,* 45(2-I), 142–150.

Samarasekara, P., & Mendoza, W.A. (2010). Effect of third order perturbation on Heisenberg Hamiltonian for non-oriented ultra-thin ferromagnetic films. *Electronic Journal of Theoretical Physics,* 7(24), 197–210.

Samarasekara, P., Abeyratne, M.K., & Dehipawalage, S. (2009). Heisenberg Hamiltonian with second order perturbation for spinel ferrite thin films. *Electronic Journal of Theoretical Physics,* 6(20), 345–356.

Spisak, D., & Hafner, J. (2005). Theoretical study of FeCo/W(110) surface alloys. *Journal of Magnetism and Magnetic Materials,* 286, 386–389. https://doi.org/10.1016/j.jmmm.2004.09.096

Usadel, K.D., & Hucht, A. (2002). Anisotropy of ultrathin ferromagnetic films and the spin reorientation transition. *Physical Review B 66:* 024419. https://doi.org/10.1103/PhysRevB.66.024419

Zhao, D., Liu, F., Huber, D.L., *et al.* (2002). Step-induced magnetic-hysteresis anisotropy in ferromagnetic thin films. *Journal of Applied Physics,* 91(5), 3150–3153. https://doi.org/10.1063/1.1433179